Bolometric Detectors for the Planck Surveyor

Minhee Yun*[a], Tim Koch[a], Jamie Bock[a], Warren Holmes[a], Leonard Hustead[a], Larry Wild[a], Jerry Mulder[a], Anthony Turner[a], Andrew Lange[b], and Ravinder Bhatia[b]

[a] Jet Propulsion Laboratory, Pasadena, California 91109
[b] Department of Physics, California Institute of Technology, Pasadena, California 91125

ABSTRACT

The High Frequency Instrument on the NASA/ESA Planck Surveyor, scheduled for launch in 2007, will map the entire sky in 6 frequency bands ranging from 100 GHz to 857 GHz to probe Cosmic Microwave Background (CMB) anisotropy and polarization with angular resolution ranging from 9' to 5'. The HFI focal plane will contain 48 silicon nitride micromesh bolometers operating from a 100 mK heat sink. Four detectors in each of the 6 bands will detect unpolarized radiation. An additional 4 pairs of detectors will provide sensitivity to linear polarization of emission at 143, 217 and 353 GHz. We report on the development and characterization of these detectors before delivery to the European HFI consortium.

Keywords: Bolometers, Millimeter-wave, Planck

1. INTRODUCTION

Planck was selected in 1996 as the Medium Mission M3 of the Horizon 2000 Plan of the European Space Agency (ESA) as shown Fig.1. Planck is dedicated to obtaining definitive images of the Cosmic Microwave Background (CMB) fluctuations and to extract the primordial signal to high accuracy from contaminating astrophysical sources of confusion. Planck will allow the precise determinations of the fundamental cosmological constants which define our Universe, including the densities of baryonic, c*[author]old and hot dark matter, the value of the cosmological constant and the Hubble constant, and the neutrino content of the Universe. Planck will use two focal plane units: a Low Frequency Instrument (LFI) using High Electron Mobility Transistors (HEMTs) sampling the frequency range 30-100 GHz and a High Frequency Instrument (HFI) using bolometers, sampling in the frequency range from 100-857 GHz. Planck will be launched by an Ariane 5 launch vehicle into a halo orbit around the L2 libration point in the Sun-Earth system in 2007. The spacecraft will be spin stabilized with a spin rate of 1 rpm. The HFI is designed to measure the temperature anisotropy and polarization of the CMB radiation over the frequency bands where contamination from foreground sources is at a minimum and the CMB signal is at a maximum. Emission from foreground contributions (from the Galaxy and extra-galactic sources) will be removed from the sky maps by measuring the spectral signature of the fluctuations over a wide frequency range.

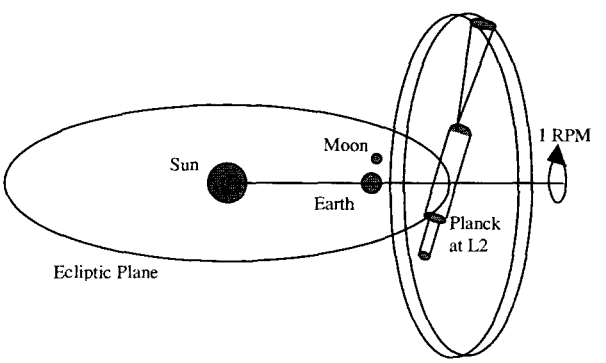

*contact, Minhee.Yun@jpl.nasa.gov; phone 1 818 354-3413

Figure 1. Planck Scan Pattern

The HFI is therefore a multiband instrument with 6 bands from 100 to 857 GHz. The focal plane is a layout of 48 bolometric channels in 36 pixels fulfilling all of the scientific requirements.

The HFI consists of (i) the HFI Focal Plane Unit (FPU), (ii) the JFET Box (iii) the Readout Electronics, (iv) the Data Processing Unit (DPU), (v) the Coolers, and (vi) harness and tubes linking various subsystems. It is based on bolometers cooled to 100 mK. Bolometers are sensitive to the heat deposited in an absorber by the incident radiation. Very low temperatures are required to obtain a low heat capacity giving high sensitivity with a short thermal time constant. Cooling the detectors at 100 mK in space is a major requirement that drives the architecture of the HFI. This is achieved, starting from the passively cooled 50/60 K stage of the payload module, by a four-stage cooling system (18K-4K-1.6K-0.1K). The 18 K sorption cooler is common to the HFI and the LFI. The 4 K stage protects the inner stages from the thermal radiation of the 20 K environment. It also provides an electromagnetic shield (a Faraday cage) for the high impedance part of the Readout Electronics. The coupling of the telescope with the detectors is made by back-to-back horns attached on the 4 K stage, the aperture of the waveguides being the only radiative coupling between the inside and the outside of the 4 K box. Optical filters are attached on the back of the 4 K horns, on the 1.6 K stage and on the 100 mK horns to provide an optimal distribution of the out of band heat loads on the different stages. The HFI focal plane unit has an extension to the 18 K and 50/60 K stages, enclosing the first stage of the preamplifiers (J-FET's). The AC bias and Readout Electronics performs all the electrical functions of the cold stages, including the temperature measurement and control. To control systematics, close-to-great-circle scans at 1 rpm are used requiring stability of the detector system on minute time scales and a speed of response <4 msec (16 mHz to 25 Hz).

In this research, we will be delivering detectors for three HFI models. Detectors with relaxed performance requirements are delivered for the Elegant Breadboard (EBB) and Cryogenic Qualification Model (CQM). Proto Flight Model (PFM) detectors of each frequency band and polarization type will fully comply with all requirements flowed down to the detectors and documented in the Business Agreement: "Detectors for the Planck High Frequency Instrument". The PFM detectors will have undergone a full program of testing, electrical calibration and verification prior to delivery to ESA.

2. DETECTOR FABRICATION

All of the silicon nitride micromesh bolometers are fabricated at JPL's Micro Devices Laboratory (MDL). The silicon nitride micromesh spider web bolometer (SWB), technology developed for Planck will provide background limited performance in all bands. The radiation is efficiently absorbed in a conducting film deposited on a micromesh absorber, which is thermally isolated by radial legs of uncoated silicon nitride that provide rigid mechanical support with excellent thermal isolation as shown Fig. 2. The use of microelectromechanical system (MEMS) techniques in this research has improved the fabrication process required for developing large-format bolometer arrays. The fabrication process must give a high mechanical yield in order to be suitable for large-format arrays. The etch technique is challenging in part because our large 300 x 100 x 25 um NTD Ge thermistor and associated In bump bonds must not be damaged during the process. NTD Ge was chosen for this application due to its extreme noise stability. The thermal conductance G, determines sets the responsivity and sensitivity of a bolometer. Therefore the fabrication process must result in uniform thermal conductivity to give uniform detector performance. Finally, the process must not result in excess heat capacity, particularly over the extended area absorber, since the speed of response of the detectors will be degraded.

In this research, we used HND (HF-HNO_3-DI Water) wet etching and deep trench reactive ion etch (RIE) technologies to fabricate the micromesh spider web bolometer. HND etching technology [1] is a very common wet process widely used for removing the damaged layer materials and cleaning surface of the materials. In addition to that, silicon wafers are typically wet etched in mixtures of nitiric acid and hydrofluoric acid. The most common dry etching technique is reactive ion etching (RIE). With RIE, ions are accelerated toward the material to be etched and the etching reaction occurs in the direction of ion travel. Deep trench RIE is an unique technique and extensively used in semiconductor field. Deep trench etching has many advantages compare to wet etching such as etch uniformity and etch profile. The difficulties in performing a successful deep trench etch process have been compounded by the range of the requirements for various MEMS applications : etch depth from 20μm to over 300μm; aspect ration of greater than 30; with silicon exposed area of below 5% to over 80% [2]. The deep trench RIE allows us to remove the bulk silicon without exposing

the sensitive layer on the front side of the detector (e.g. In, Ge, Ti) to reactive etchants. The buried oxide layer also prevents fluorine-based etch products from contacting any portion of the active area of the detector. We selected the HND liquid etch as the second step of the etch process, because we found that the deep trench RIE process left significant residues with large excess heat capacity when the active area of the bolometer was directly exposed to the etch. The liquid etch step produces devices with low heat capacity, but unfortunately also results in lower device yield.

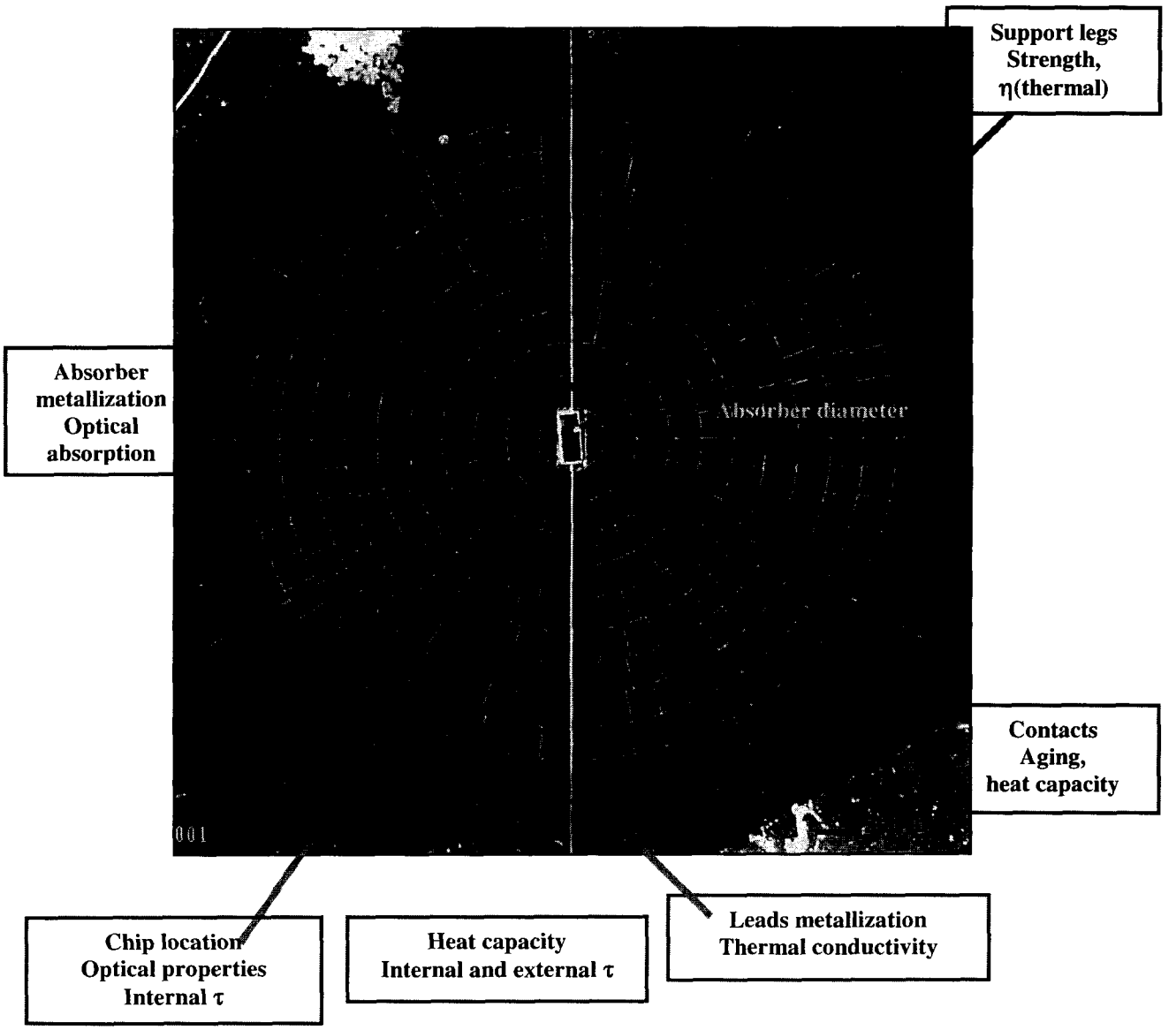

Figure 2. Spider web architecture with NTD Ge thermometer.

The temperature of the absorber is measured by small (25x100x300 um) neutron transmutation doped (NTD) Ge thermistor that is indium bump bonded to and read out with thin film leads that are photo-lithographed on two of the radial legs. Compared to a solid absorber, the micromesh has a geometric filling factor of only ~1.5%, providing a correspondingly small suspended mass, absorber heat capacity and cosmic-ray cross-section. Micromesh bolometers are currently used in numerous CMB experiments (BOOMERANG, MAXIMA, SuZIE, Archeops) which operate under

similar optical loading and detector sensitivity requirements to those needed here. Each polarization sensitive detector uses a pair of a new type of bolometer. These Polarization Sensitive Bolometers (PSB's) use identical fabrication processes as the SWB but have a new absorber geometry that makes them sensitive to only one linear polarization.

The process sequence of the fabrication of SOI micromesh spider web bolometer is shown in Fig. 3. These processes, including cleaning, dry etching, LPCVD (low pressure chemical vapor deposition), lithography, and metallization, are standard semiconductor fabrication techniques. The wafers used in this research were thermally bonded SOI wafers with (100) orientation. The thicknesses of the top Si, buried SiO_2, and bottom Si layer were 2 μm, 1 μm, and 350 μm, respectively, with ±10% variation. One of advantages of using SOI material is that reduces the total chip size compared to standard bulk micromachining because of buried oxide. First, the SOI wafers were prepared with standard RCA cleaning. Then, 1 μm layer of Si_3N_4 [Fig. 3(a)], which acts as support legs, was deposited on the wafer using low-pressure chemical vapor deposition (LPCVD). Several Au depositions using photolithography processes form the absorber for optimal infrared absorption, the electrical leads which define the thermal conductance, and the wiring layer for electrical readout. Ti-Au metal films are deposited using lift-off technique to form the absorber layer [Fig. 3(b)]. The thickness of the Au layer deposited on the absorber is chosen to give optimal infrared absorption. The thickness of the Au layer forming the electrical leads on the supports may be varied to tailor the thermal conductance. The thickness of electrical contacts of the array was formed from a 5 nm Ti + 500 nm Au film [Fig 3(b)]. The wafer is then patterned to define the mask for the membrane [Fig. 3(c)], and etched first with an Ar reactive ion etch to remove the absorber Ti-Au layer followed by a CF_4 and O_2 reactive ion etch to remove the silicon nitride. The backside is similarly patterned, aligning to the frontside with an infrared camera, and reactive ion etched to remove the backside silicon nitride to define the silicon frame [Fig. 3(d)]. A 15 μm x 40 μm Ni-In bump [Fig. 3(e)] is deposited on each of the two contact pads located at the center of the device using liftoff lithography to deposit 40 nm Ni + 3 μm In. The nickel layer is used as an intermediate layer to prevent reaction of the indium with the gold during processing. The arrays are diced into a hexagonal shape from the original wafer. Before attaching the thermistors, the backside is patterned with photoresist and hard baked at 130 °C for 5 minutes. The thermistors are manufactured from a polished slab of NTD Ge material by p doping with a 4.53 x 10^{16} /cc concentration of Ga and a 1.29 x 10^{16} /cc compensation of As. Two contacts are defined on a single face of the chip by photolithography. The contacts are B-implanted and deposited with 2 nm Ti + 20 nm Au. Two 15 μm x 15 μm In bump bonds are then patterned on each contact of the thermistor with the same Ni-In process used on the wafer. The chips are diced with a diamond saw and etched in a mixture of HF and HNO_3 to remove saw damage. The resulting chips are ~300 μm long, ~50 μm wide, and 25 μm thick with two contacts 100 μm wide and 50 μm long, separated by 200 μm. The NTD Ge thermistor was located [Fig. 3(e)] over the contacts at the center of the absorber and attached by the In bumps with 1 - 2 N of force by a micrometer. Finally the silicon was removed using a deep trench reactive ion etch to the insulating layer [Fig. 3(f)], followed by liquid etches to remove the thin oxide and silicon layers [Fig. 3(g)]. We have used ICP (inductive coupling plasma) system for deep trench etching because ICP appears to be the most suitable source for this application. This system allows high etch rates, anisotropic etching with selectivity to conventional photoresist masks [3]. Deep reactive ion etcher (DRIE) is manufactured at Surface Technology Systems (STS) and is a single wafer, load locked system that employs inductively coupled plasma etching with the Advanced Silicon Etch (ASE) process. The plasma was generated by inductive coupled coil by 13.56 MHz with a maximum power output of 1000W. Another 13.56 MHz generator is used to apply the electrode which allows independent control of the bias potential of the wafer with a power up to 300W. The wafer temperature is maintained less than 80°C via temperature controller which is connected to LN_2 supplier. The system and reaction pressure is controlled by APC (automatic pressure controller). Typical base pressures are 1 x 10^{-7} Torr and operating pressures are from 1 mTorr to above 10 mTorr. During processing, the wafer electrode is lifted using a large bellows from loading height to a processing height within 10 mm of the bottom coil. This reduces ion density loss by diffusion. The electrostatic chuck and platen assembly are cooled by a de-ionized water chiller system. Wafer cooling is provided by mass flow controlled helium on the backside of the wafer. Ion densities of the order of 10^{12} cm^{-3} are obtained at the center of the chamber. We have used SF_6 and C_4F_8 as the etch and passivation gases respectively. SF_6 is used during etch step to etch Si isotropically, this is followed by a short passivation step using C_4F_8. The SF_6 gas provides fluorine radicals which are the isotropic silicon etchants. The C_4F_8 plasma deposits a polymeric passivating layer on surface as well as side wall [3]. The directional ion energy supplied by the capacitive coupled electrode during the etch reaction preferentially removes the paasivation layer from the base of the features hence etching silicon spontaneously. The balance between etch and passivation determines the final process results and this balance can be controlled through a wide variety of process parameter such as etch time RF power, gas flow, and etch pressure.

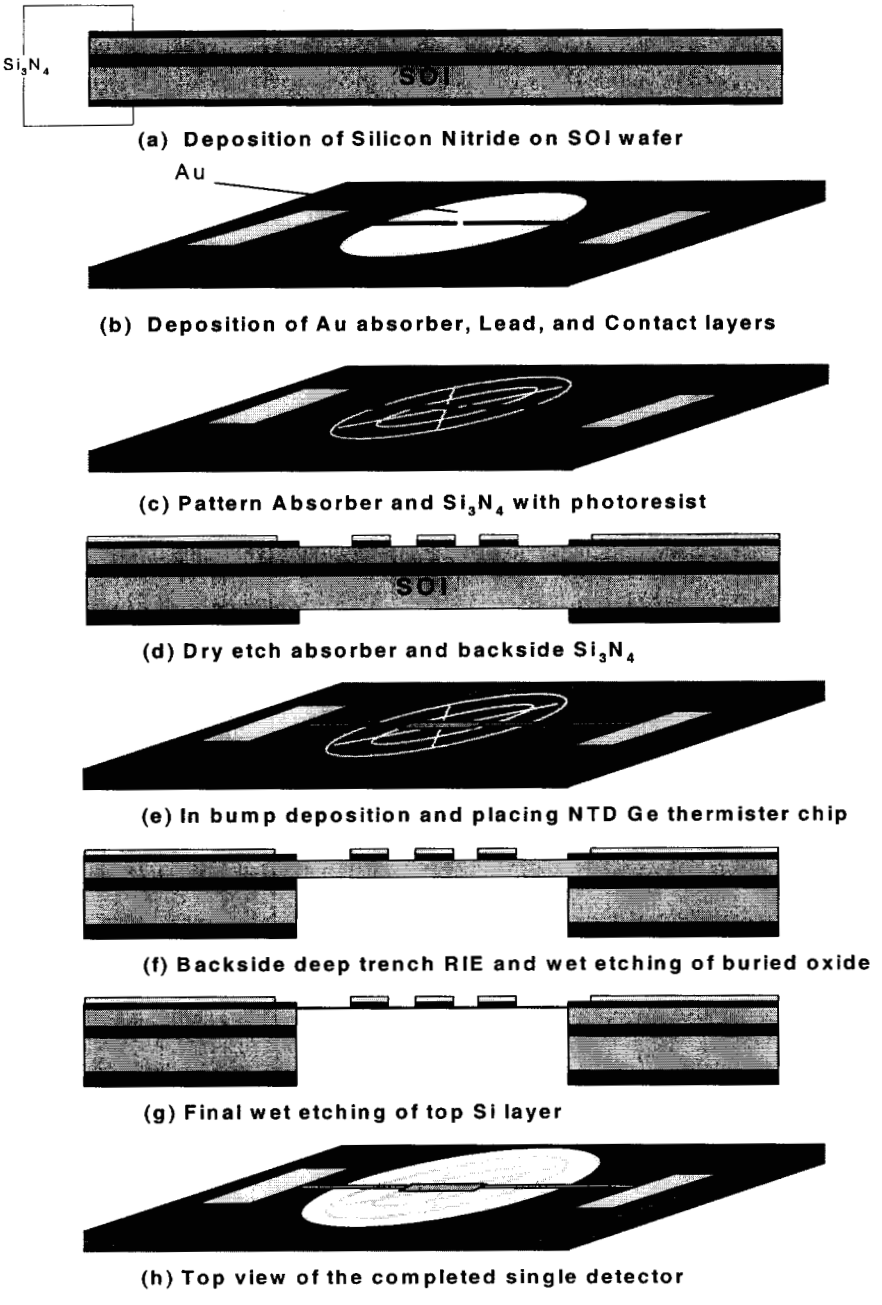

Figure 3. Process Flow Diagram

The etch reaction starts with introducing standby step which consists of high purity N_2 purge followed by a system pumping out. Then etching gases of 130 sccm of CF_4 and 85 sccm of C_4F_8 are introduced using mass flow controller. The etch rate in this system was 2.2 μm/minute. It varies a little depending upon exposed surface area and feature size. In general, to etch through bottom silicon layer, a 350 micron, takes about 160 minutes. The selectivity to etching relative to silicon is 150 : 1 for the oxide and 75 : 1 for the photo resist. The etch process stopped when silicon has cleared. After the final etch, the standby step is repeated and the load lock handler removes the wafer from the reaction chamber. Fig. 3(h) shows the final single spider web array after releasing and cleaning. Each bolometer Si_3N_4 support legs are 5 μm wide and 1 μm thick. The web legs are 4 μm wide and 1μm thick leading to a filling factor of approximately 1.5% in each element of the array. This small filling factor over such a large area allows highly energized

particle to pass undetected while still capturing the wavelength of radiation being observed. The absorber has a relatively small mass and is suspended by support legs of silicon nitride which provides robust mechanical support and very low thermal conductivity. Therefore the fabricated bolometer device is mechanically insensitive to the relatively low frequency vibration encountered during launch and operation. Figure 4 shows a completed spider-web bolometer module after packaged at JPL packaging lab.

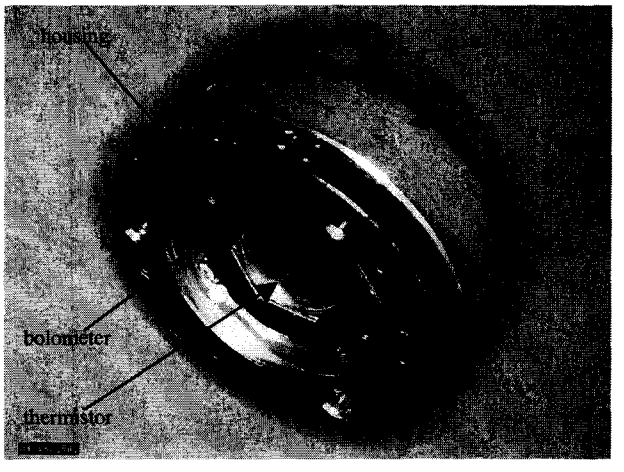

Figure 4 SWB Module

3. CHARACTERIZATION

3.1 Thermal Environment

Because the HFI bolometers operate at 100 mK, an Oxford Instruments Kelvinox-25 ^{3}He/^{4}He dilution refrigerator has been instrumented to perform the necessary low temperature characterization of the detectors as shown Fig. 5. The test facility is capable of testing up to 21 bolometers per run. All channels have demonstrated intrinsic electronic noise <6 nV/$\sqrt{\text{Hz}}$ over the frequency range 0.010 to 25 Hz, and individual bolometers delivered for use in the flight program have been measured to have <12 nV/$\sqrt{\text{Hz}}$ intrinsic noise under biased conditions in the absence of illumination. The thermal stability required for bolometer intrinsic noise determination is 40 nK/$\sqrt{\text{Hz}}$ from 0.016 to 25 Hz. This is implemented via passive thermal design and active feedback using high resolution thermometry. A four stage structure provides passive thermal filtering. Active control of a stage distributes the thermal noise power density over a wider bandwidth and modulation of the isolated stage where the detectors are mounted is reduced.

3.2 Optical Excitation: speed of response measurement

A bolometer's heat capacity (C~1 pJ/K) and the thermal conductance (G~100 pW/K) of the link to the 100 mK thermal reservoir determine the speed of response. This bolometric response is modified from simple $\tau = C/G$ (~10 ms) by the weak electrothermal feedback of the thermistor, but essentially behaves as single pole rolloff. In order to measure the response to variable-frequency, constant-amplitude input radiation, a light pipe transports radiation from source outside the dewar at 300 K to bolometers at 100 mK via a thin-wall stainless steel tube, gold-plated on the upper section. This technique has demonstrated the optical response of bolometers under conditions similar to those expected in flight.

3.3 Vibration Testing

Specialized fixturing holds up to three (3) "slices" of 8 bolometers per test run in a hermetic volume, opened only under controlled conditions. The vibration tests are preformed at JPL.

3.4 Thermal Cycling

An LN2 cryogen dewar has been modified with a sample holder that can hold two (2) "slices" of 8 bolometers, a variable flow heat exchanger and heaters. Automated operation allows unattended thermal cycling between 330 K and 80 K. The resistance of each bolometer is recorded throughout the cycling intervals to a precision of 1%.

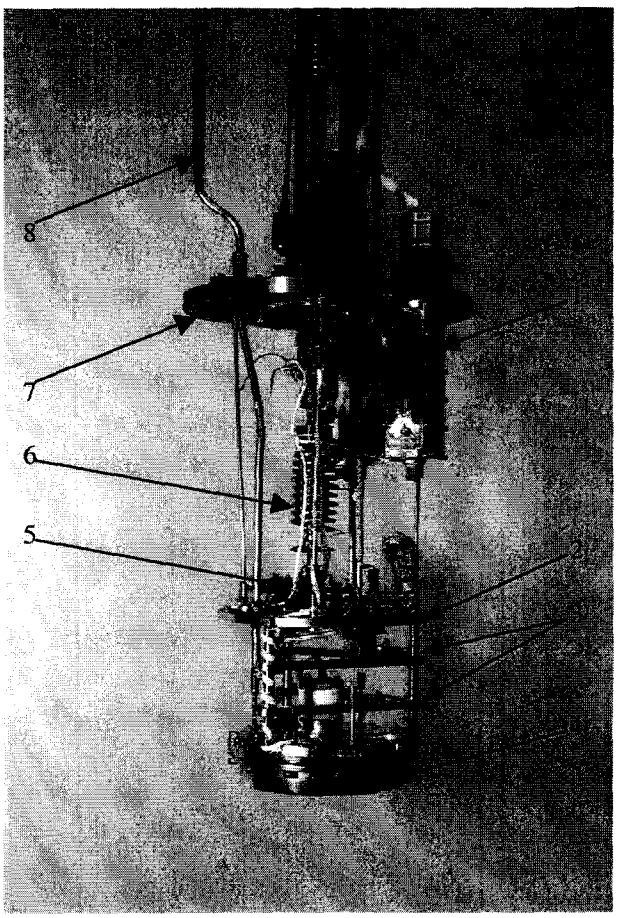

Figure 5 100 mK Test Bed: 1) JFET box; 2) 100 mK cold plate; 3) passive thermal filter stages; 4) evacuated sample can; 5) ^{3}He/^{4}He mixing chamber; 6) heat exchanger; 7) indium vacuum to LHe seal; 8) light pipe.

3.5 Qualification

Qualification Testing is performed on devices which have completed flight Acceptance Testing after which they are not flight deliverables. Twelve (12) detectors, 6 SWB (6 bolometers) and 6 PSB (12 bolometers), are taken as a representative sampling. Acceptance Performance Tests will then be repeated on all devices and the results will be evaluated for a Qualification report. The simple construction of the detectors allows us to qualify the entire assembly as a hybrid. The number of cryogenic thermal cycles for Qualification, 80, was chosen based on the estimates from various of our collaborators, indicating that the total number of cycles to cryogenic temperatures likely to be experienced by the Flight devices is ~25. The choice of cycling to a low temperature of ~90 K (LN2), rather than to the operating temperature of 100 mK or to 4.2 K (LHe), is based upon experience with similar devices which indicates that most failures occur during transition within this temperature range, and on general experience within the low temperature community that the majority of damage due to differential thermal contraction occurs within this temperature range. Additional detectors will undergo Accelerated Aging (1000 hours, 85% RH, 70 C). Resistance will be monitored

continuously. We have determined that the elevated temperature is not detrimental, however, we will be able to set limits on exposure to elevated humidity and take steps to control it.

4. DEVICE PERFOMANCE

Table 1. Required Bolometer Performance

Frequency [GHz]	g [μm]	2a [μm]	d [μm]	ff [%]	C [pJ/K]	G [pW/K]	NEP [e-17W/rtHz]
100	320	4.8	4500	3	0.94	120	1.27
143	225	3.4	3160	3	0.59	160	1.37
217	160	2.4	2280	3	0.42	215	1.65
353	160	2.4	2280	3	0.42	215	2.08
545	110	6.4	2200	1.16	0.41	250	5.21
857	70	4	2100	11.4	0.39	1590	14.3

g, grid spacing; 2a, line width in absorber; d, absorber diameter of active area; ff, absorber filling factor; C, required heat capacitance; G, required thermal conductivity; NEP, required noise equivalent power

We have fabricated free-standing Si_3N_4 micromesh with a wide variety of geometries dependent on various frequencies as shown Table 1. In the absorber, the widths of legs are 4.5μm, 3.4μm, 2.4μm, 2.4μm, 6.4μm, and 4μm for 100GHz, 143 GHz, 217 GHz, 353 GHz, 545 GHz,, and 857 GHz, respectively. We have designed grid spacing as small as 70μm and as large as 320μm. The thickness and width of the support legs are 1μm and 5μm. Active areas of the absorber were designed from 3.46mm^2 to 15.9mm^2. The filling factor of the absorber is between 3% and 11.6%. The required heat capacities for each frequency are listed in Table1 showing between 0.39pJ/K for 857GHz and 0.97pJ/K for 100GHz. The active area and the thermistor may dominate for the heat capacities at 100mk from previous report [4]. We have measures heat capacities as a function of the absorber area as shown Fig. 6. The heat capacities show between 0.96pJ/K and 1.92pJ/K for 100GHz bolometers, and between 0.24pJ/k and 3.03 for 143GHz, and between 0.30pJ/K and 1.90pJ/k for 217GHz, and between 0.23pJ/K and 2.15pJ/K. The study of heap capacities for 545GHZ and 857GHz are on going.

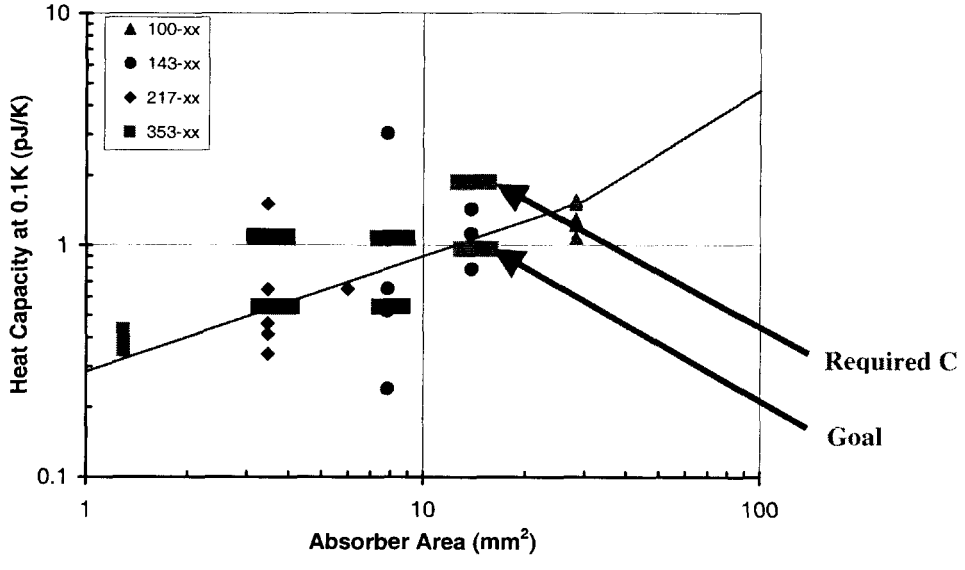

Figure 6. Measured Heat Capacities Showing Required and Achieved

From these measurements, we may need to select good bolometers to meet specifications required from ESA. We are investigating whether excess heat capacities come from absorber or process. The preliminary results of thermal conductance properties dependent on lead impedances at room temperature are given in Figure 7. Thermal conductivity across the absorber could result a loss in optical responsivity. The conductivity between absorber and heat sink is more than 1 order of magnitude smaller than the thermal conductivity of the nylon supports used in other low background composite bolometers at 300mK, which allows Si_3N_4 micromesh bolometers to achieve higher sensitivity under low-background conditions[5]. The internal thermal conductivity of the absorber is corresponding to the conductivity of single leg in the central active area and has contributions from both the metal film and the silicon nitride. The thermal conductivity of the metal is related by the Wiedemann-Franz law to the electrical conductivity required for absorption and dominates over the silicon nitride at lower than 300 mK temperature.

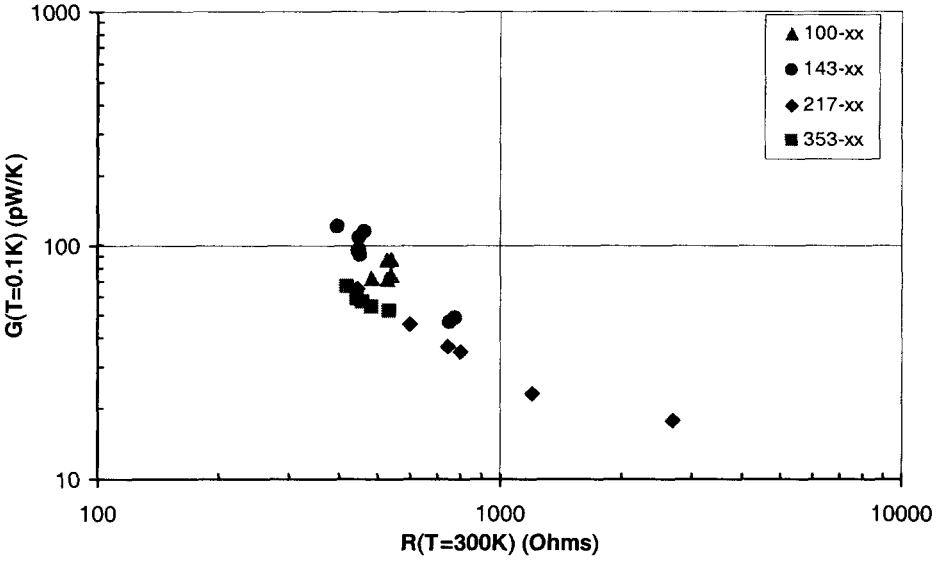

Figure 7. Measured Thermal Conductivity Dependent on Lead Impedance

As shown Figure 7, measured thermal conductivities of silicon nitride micromesh bolometers range from 17.7pW/K fro 217GHz and 120.67pW/K for 143GHz. Because thermal conductivity of these bolometers is dominated by lead impedance, we used thin Au/Ti layer up to 750Å dependent on frequency. We built a bolometer with 5μm width and 470 Å of Au/Ti with a G = 17.7pW/K. All other measurements such detecting time constant and NEP measurements are on going at present time.

5. SUMMARY

We have developed and fabricated Si_3N_4 micromesh bolometers to obtain definitive images of the Cosmic Microwave Background (CMB) fluctuations and to extract the primordial signal to high accuracy from contaminating astrophysical sources of confusion for Planck mission. The strength of the scientific case for Planck is recognized both in Europe and in the USA. The detection of CMB anisotropies in 1992 by NASA's Cosmic Background Explorer (COBE) has opened up an entirely new way of studying cosmology to high precision. With the successful launch of the Microwave Anisotropy Probe (MAP) in June 2001, the next decade will see enormous experimental effort dedicated to mapping the CMB at increased sensitivities and angular resolution. Planck is the third generation CMB mission, after COBE and MAP, and will obtain definitive images of the CMB fluctuations and will be able to extract primordial signal to high accuracy from the contaminating astrophysical sources of emission. This can be achieved by Planck which combines high resolution, high sensitivity ($dT/T < 3x10^{-6}$ in each 7 arcmin pixel), wide frequency coverage and excellent control of systematic errors. This combination of requirements cannot be met either by ground-based or balloon-borne observatories and demands a space mission such as Planck.

ACKNOWLEDGMENTS

We would like to thank MDL researchers at JPL for their useful discussions regarding to the process development. We also thank Rick Vasquez and Judy Podosek in their valuable contribution to Planck.

REFERENCES

1. E. S. Kooji, K. Butter, and J. J. Kelly, Electrochemical and Solid-State Letters, 2(4), 178(1999)
2. J. Bhardwaj and H. Ashraf, Proc. Micromachining and Microfab. Pro. Tech., SPIE, 2639, 224(1995)
3. A. M. Hynes, H. Ashraf, J. K. Bhardwaj, J. Hopkins, I. Johnston, and J. N. Shepherd, Sensors and Actuators, 74, 13(1999)
4. P. D. Mauskopf, J. J. Bock, H. Del Castillo, W. L. Holzapfel, and A. E. Lange, Applied Optics, 36(4). 765(1997)
5. J. J. Bock, J. Glenn, S. M. Grannan, K. D. Irwin, A. E. Lange, H. G. Leduc, and A. D. Turner, Pro. Adv. Tech. MMW, Radio, and Terahertz Telescopes, SPIE, 3357, 297(1998)